Effects of adding trace amounts of Mn on grain boundaries in improving the PTC properties of $Ba_{0.99}Y_{0.01}TiO_3$ ceramics

MAOLIN ZHANG[a,*], TONGTONG XUE[a], ZHIMIN LI[a], YANGXI YAN[a], ZI YANG[a], YUNXIA HUANG[a], JINBIAO PANG[b]
[a]*School of Advanced Materials and Nanotechnology, Xidian University, Xi'an, 710071, P.R. China*
[b]*China Zhenhua Group Yunke Electronics Co., Ltd, Guiyang, 550018, P.R. China*

Barium titanate ($BaTiO_3$) is a typical positive temperature coefficient (PTC) ceramic which is closely associated with the state of grain boundary. In this work, $Ba_{0.99}Y_{0.01}TiO_3$ powder was obtained by the solid-state reaction method and then trace amounts of Mn (0.09~0.19%) were added to promote the direct interaction with grain boundaries. The effects of trace Mn on crystal structure, microstructure, binding energy and PTC characteristics were investigated. It was found that excellent room-temperature resistivity, resistance jump ratio and Curie temperature of 136 Ω. cm, 10^5 and 145 °C, respectively, could be obtained for the 0.11% Mn-doped ceramics, possibly due to the grain boundary barrier induced by Mn.

(Received October 5, 2016; accepted June 7, 2017)

Keywords: Barium titanate, PTC ceramic, Grain boundary, Trace Mn

1. Introduction

Barium titanate ($BaTiO_3$) is a perovskite-type ferroelectric ceramic material which displays positive temperature coefficient resistivity (PTCR) effect. The barium titanate-based ceramics show an anomalous increase in electrical resistance over a small temperature interval (Curie temperature, T_c) [1]. These materials have been widely used in several electric devices, including current control elements, over-current protection devices, self-controlled heaters and so on [2-3]. These applications of the ceramics mainly focus on their electrical properties, such as room temperature resistance (R_{25}), resistance jump ratio (R_{max}/R_{min}) and Curie temperature (T_c).

It is known that the most effective way of increasing the grain electronic conductivity of a semiconducting ceramic is by acceptor or donor doping. Usually, dopants such as Ni^{2+}, Y^{3+}, La^{3+} and Nb^{5+} ions are doped into $BaTiO_3$ ceramic to improve the room temperature conductivity [2, 4-5]. Gong et al. [6] doped Y into a $BaTiO_3$-based PTC ceramic through sol-gel method. By controlling the content of impurity, the room temperature conductivity showed a rapid increase. The mechanism involved in the improvement of resistance degradation for Y-doped $BaTiO_3$ ceramic has been discussed by Sato et al. [7]. The results indicated that the Y^{3+} ion substituted for perovskite A-site and acted as donor. Masayoshi et al. [8] prepared La-doped $BaTiO_3$ through solid-state method and oxalic acid method to decrease the room temperature resistance. It was found that the room temperature resistivity could be lowered to below 50 Ω.cm and the resistance was strongly affected by the preparation route of La-doped $BaTiO_3$, owing to the differences in micro-structures and acceptor states at the grain boundaries. Yang et al. [2] found that extra doping with an appropriate amount of Nb_2O_5 in $BaTiO_3$-$Bi_{0.5}Na_{0.5}TiO_3$ ceramics could neutralize the redundant acceptor of Na^+ ions.

On the other hand, it is well known that the PTC effect is mainly associated with the ferroelectric to paraelectric phase transition and the development of resistive barriers at the grain boundaries [9-10], which results in an anomalous increase in electrical resistance of several orders. Over the last few decades, the first suggestion that the resistivity jump was caused by increase in the grain boundaries was made by Heywang in 1964 [11]. Since then, Daniels [12], Jonker [13], Desu [14], and several other scholars have extended Heywang's model, gradually approaching the physical essence of the PTC effect. According to their models, surface acceptor states present at grain boundaries are responsible for the formation of electron depletion layers and the potential barrier [8].

Several previous works have proposed the appropriate phase, composition and microstructure of grain boundaries and even the preparation methods to adjust the grain boundary conditions, in order to improve the PTC effect [15-20]. Acceptors such as Mn^{2+} and Cu^{2+} ions segregated at the grain boundaries have been used to improve the PTC effect [16]. Moreover, additive agents such as SiO_2 have also been introduced to adjust the states of grain boundaries by Leach [17-18] and Pu [1]. Huo et al. [19] doped CuO in $BaTiO_3$-based PTC ceramics. The result showed that the PTC effect was improved with 0.1 mol% CuO, and the magnitude of the PTC effect was increased up to 10^6. However, the PTC effect disappeared when the doped content of CuO increased to 1%. Qian et al. [20] doped Mn^{2+} ions into a $BaTiO_3$-based PTC ceramic by solid state reaction and used EPR spectroscopy to analyze the ceramic. The results showed that the g factor and hyperfine splitting constants corresponded to the different phases of Mn-doped $BaTiO_3$. According to Paunovic's [4] work, Mn was used as an acceptor dopant incorporated at Ti^{4+} site, in order to counteract the influence of the oxygen vacancies and prevent exaggerated grain growth. However, all these studies gave resistivity values of above 10^{10} Ω. cm.

In this work, Y^{3+} ions were used as donors in the $BaTiO_3$ ceramic to increase the grain electric conductivity [21-22]. Furthermore, Mn was introduced to improve the resistance jump ratio [10, 16, 20]. However, Mn does not need to be introduced in the starting materials to perform the role of acceptor. Instead, in order to adjust the grain boundary condition and change its electrical performance, a trace amount of Mn was added to promote the direct interaction with grain boundaries, after the $Ba_{0.99}Y_{0.01}TiO_3$ precursor ceramic powder was obtained by pre-sintering. The effect of adding trace amounts of Mn on grain boundaries, and the mechanism involved in improvement of the PTC properties of $Ba_{0.99}Y_{0.01}TiO_3$ ceramics were investigated in depth.

2. Experimental details

2.1. Ceramic fabrication

The $Ba_{0.99}Y_{0.01}TiO_3$ ceramic powders were prepared by the conventional solid-state reaction technique in air atmosphere. Analytically pure reagents, including $BaCO_3$, TiO_2, Y_2O_3 and SiO_2 powders were used as the starting materials.

Firstly, the starting materials were weighed at a molar ratio of Ba: Ti: Y: Si=0.99: 1: 0.01: 0.02 and mixed by wet ball milling for 8 h. Then, the mixture was dried and calcined at 1150 °C for 150 min to obtain the $Ba_{0.99}Y_{0.01}TiO_3$ precursor.

Secondly, $Mn(NO_3)_2$ solution was used to modify the grain boundary of prepared $Ba_{0.99}Y_{0.01}TiO_3$. The as-synthesized $Ba_{0.99}Y_{0.01}TiO_3$ and trace amounts of $Mn(NO_3)_2$ solution were weighed according to the composition of $Ba_{0.99}Y_{0.01}TiO_3$-$xMn(NO_3)_2$ with x=0.09%, 0.11%, 0.13%, 0.16% and 0.19%. The mixtures were then ball-milled for 8 h in alcohol. After drying and granulating with 6 wt% polyvinyl alcohol (PVA) as binder, the powders were pressed into disks at a pressure of 5 MPa and then sintered at 1300 °C for 120 min in air. A PTC ceramic disk with 2 mm thickness and 8.8 mm diameter was formed. The samples with trace amounts of $Mn(NO_3)_2$ (0.09%-0.19%) were labeled as M_1-M_5, respectively.

Finally, electrodes were fabricated on both surfaces of the ceramic in order to measure the electrical properties. Aluminum paste was screen printed on both surfaces of the disks, and sintered at 550 °C for 30 min to obtain ohmic contact between electrodes and ceramics.

2.2. Characterization

X-ray diffraction (XRD, D/MAX-2400, Rigaku, Japan) was used to identify the phase composition and lattice parameters of the PTC ceramics at room temperature using Cu Kα radiation. The XRD analyses were carried out over a 2θ range from 20° to 70° at a step size of 0.02° (2θ) and a scan rate of 0.12° s^{-1}. The microstructures of the ceramic samples were studied by scanning electron microscope (SEM, JSM-7500F, Jeol, Japan). The elemental analysis was performed on the ceramic sample's cross-section by using SEM equipped with energy dispersive X-ray analysis spectrometer (EDS, X-Max50, Oxford, UK). The resistance-temperature (R-T) properties were investigated by the resistance-temperature characteristic test system (ZWX-B, Huazhong University of Science and Technology, China), over the temperature range from room temperature to 230 °C with a rate of 5 °C/min. In addition, the complex impedance spectrum of the PTC ceramic was measured by the Vector Network Analyzer (4294A, Agilent, USA) from 40 Hz to 100 MHz.

3. Results and discussion

Fig. 1 shows the typical XRD patterns of Mn modified $Ba_{0.99}Y_{0.01}TiO_3$ ceramics. It was found that all the ceramics maintained the typical perovskite structure ABO_3 (JCPDS#75-0462) and all the diffraction peaks were similar to that of $Ba_{0.99}Y_{0.01}TiO_3$, which is in good agreement with Han's conclusions [22]. On the other hand, when the $Mn(NO_3)_2$ containing solution was heated up to the thermal decomposition temperature of 200 °C, it generated NO_2 and MnO_2. However, no secondary phase could be detected, which indicates that a trace amount of Mn cannot change the phase structure.

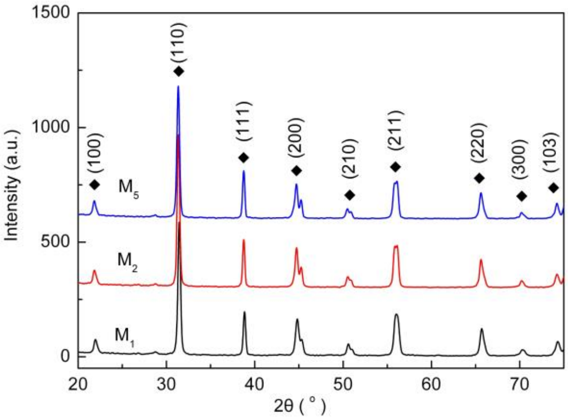

Fig. 1. X-ray diffraction patterns of M_1, M_2 and M_5 ceramics

It is well known that the PTC effect is dominated by the grain boundary. In order to ascertain the effects of micro-Manganese segregated at the grain boundaries, SEM micrographs and EDS spectra of the cross-section of the grain boundary on the $Ba_{0.99}Y_{0.01}TiO_3$-0.11%Mn ceramic were obtained, as shown in Fig. 2. Elemental mapping is shown on the EDS spectrum, and the percentage of atom fraction of all the elements is displayed on the spectrum. From the distribution of elemental mapping and the analysis of cross-section, it is found that trace amounts of Mn ions were enriched along the grain boundaries, which is the desired result.

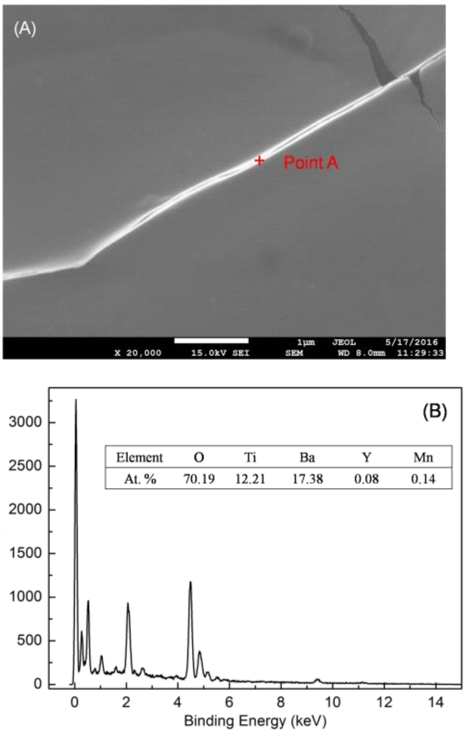

Element	O	Ti	Ba	Y	Mn
At. %	70.19	12.21	17.38	0.08	0.14

Fig. 2. SEM micrograph (A) and EDS spectrum (B) of polished cross-section of ceramic M_2 at grain boundaries

Fig. 3 shows the temperature dependence of resistivity of the prepared PTC ceramics with different Mn contents. Various amounts of Mn were added to $Ba_{0.99}Y_{0.01}TiO_3$ ceramics to determine the optimum concentration. Through the R-T characteristic tests, it can be seen that all samples exhibited a significant PTC effect, with resistance jump ratio (R_{max}/R_{min}) of 5 orders of magnitude. Here, the resistance jump ratio (R_{max}/R_{min}) was defined as the ratio of the maximum resistance after phase transition (R_{max}) to the minimum resistance before phase transition (R_{min}), and was therefore a pure number. It was also found that the resistance jump ratio increased with an increase in the amount of Mn. These results indicate that as the amount of Mn increases, the grain boundary effects are enhanced and the PTC effects are more obvious.

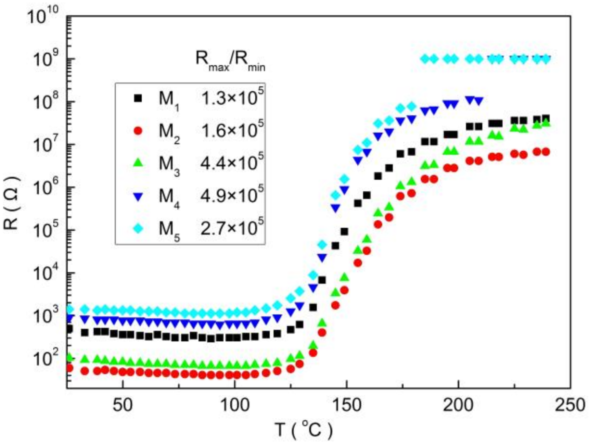

Fig. 3. Temperature dependence of resistance for different PTC ceramics

In essence, the PTC effects are grain boundary effects. It is well known that Mn ions are often doped into ceramic materials to improve the PTC effect. There are two possible reasons for this beneficial effect of Mn [23]. On the one hand, segregation of micro-Manganese enhances the adsorption of oxygen along the grain boundaries, thus improving the interface acceptor state. When segregated at the grain boundary, Mn ions tend to form an acceptor barrier which prevents the growth of grain, and increases the grain number. On the other hand, it is likely that a portion of Mn^{2+} ions replaced the vancancy of Ti^{4+} ions to improve the interface acceptor state above the Curie temperature, thus increasing the PTC effect. The anomalous increase in resistivity of all the samples was exhibited at the Curie temperature and an excellent PTC effect was observed with a resistivity jump of five orders of magnitude.

Generally, the total resistance (R_T) of a semiconducting ceramic can be divided into R_g (resistance of grain) and R_b (resistance of grain-boundary) [3, 24-26]. In order to ascertain the effects of Mn on the resistivity of grains and grain boundaries, impedance spectroscopy was performed on the $Ba_{0.99}Y_{0.01}TiO_3$-xMn (x=0.09-0.19%)

ceramics, and the results are shown in Fig. 4. An equivalent circuit model is also introduced to analyze the complex impedance characteristics of the ceramics. The impedance of the sample for different angular frequencies (ω) can be expressed using the following formula [3]:

$$Z = R_g + \frac{R_b}{1+i\omega C_b} = R_g + \frac{R_b}{1+\omega^2 C_b^2} - i\omega \frac{R_b C_b}{1+\omega^2 C_b^2} = Z' - iZ'' \quad (1)$$

Obviously, when angular frequency is 0, Z'= R_g+R_b and when angular frequency is infinite, Z"= R_g. Accordingly, the resistance of grains and grain boundaries can be calculated from Fig. 4 by a semicircle-fitting method.

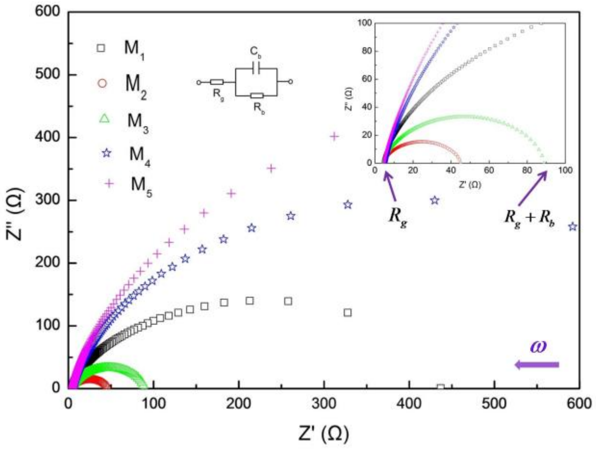

Fig. 4. The Cole-Cole circles of different ceramic samples measured at room temperature

By calculating the resistance of grains and grain boundaries, it was found that the resistance of grains (R_g) remained almost unchanged, as shown in Fig. 5. According to Han's [22] work, Y substituted for the Ba site and the equilibrium conductivity showed donor-doped behavior. In other words, there was electronic compensation and the semiconducting behavior could be explained as follows:

$$Y_{Ba}^{\times} \rightarrow Y_{Ba}^{\bullet} + e' \quad (2)$$

This indicates that the conductance may be derived from the semi-conductivity of grains, which was induced by ionization of Y in sintered PTC ceramics. When the concentration of Y is uniform in every ceramic sample, the resistance of grains (R_g) is almost the same and there is no significant change in the R_g value around 4 Ω.

On the other hand, the resistance of grain boundaries (R_b) varied significantly with increasing content of Mn. Noticeably, when the Mn content exceeded 0.11% (M_2), the number of the acceptor states at grain boundaries increased, resulting in a reduction of room temperature conductance. Noticeably, the grain boundary resistance (R_g) of M_2 (0.11%) was only 40 Ω and the resistivity of the whole ceramic was below 136 Ω.cm at room temperature. Based on the research of Pu [1], when Mn ions were doped into $BaTiO_3$ ceramic, they made the $BaTiO_3$ lattice structure more closely packed. In the presence of Mn, the diffusion of oxygen ions could be prevented from the internal lattice, which led to an increase in the grain boundary barrier.

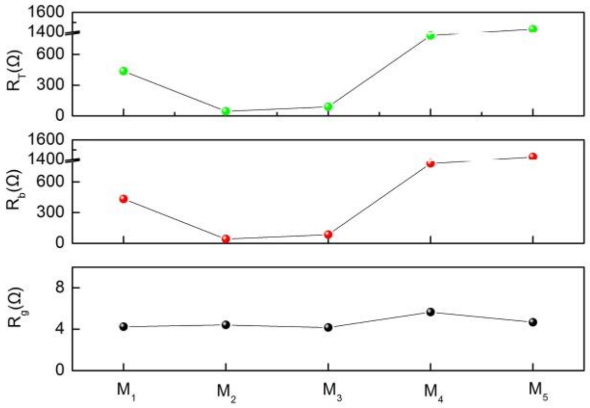

Fig. 5. R_q, R_b and R_T dependence of different ceramic samples, which were calculated from Cole-Cole circles

The Curie temperatures of the prepared PTC samples are shown in Fig. 6. It can be clearly observed that the Curie temperature decreased from 149 °C to 91 °C with an increase in the amount of Mn. According to Zhang's work [23], when the operating temperature is above the Curie temperature, Mn^{2+} segregated at the grain boundaries may transform to Mn^{3+}, as shown below:

$$Mn^{2\bullet} \rightarrow Mn^{3\bullet} + e' \quad (3)$$

The Mn^{3+} was regarded as an acceptor to replace the Ti^{4+} atom, which led to an increase of interface acceptor density state. Accordingly, sample M_1 with the least amount of Mn exhibited the maximum Curie temperature, 149 °C.

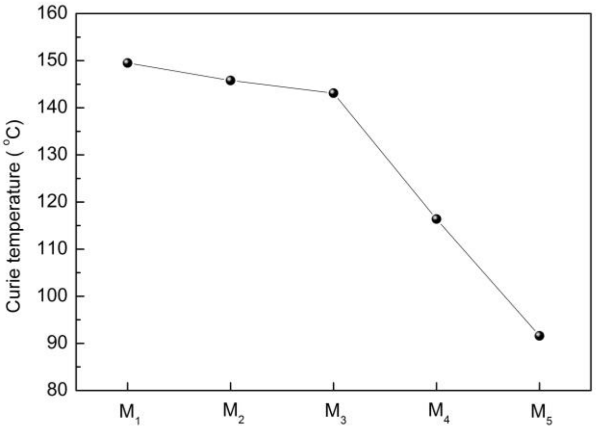

Fig. 6. The Curie temperature of different ceramic samples

4. Conclusions

In this work, $Ba_{0.99}Y_{0.01}TiO_3$-xMn (x=0.09%~0.19%) PTC ceramics were fabricated by the conventional solid-state reaction method. It was found that the resistance of grains (R_g) remained almost unchanged (4 Ω) possibly due to the Y^{3+} ions acting as donor. The incorporation of trace amounts of Mn ions into the grain boundary could not change the structure and morphology of $Ba_{0.99}Y_{0.01}TiO_3$. Instead, the trace amounts of Mn ions were enriched along the grain boundaries building the grain boundary barrier. As a result, excellent electrical properties with room-temperature resistivity, resistance jump ratio and Curie temperature (Tc) of 136 Ω. cm, 10^5 and 145 °C, respectively, could be obtained with the M_2 ceramic sample.

Acknowledgements

This work was supported by the Specialized Research Fund for the Doctoral Program of Higher Education [grant number 20130203120016]; the Natural Science Basic Research Plan in Shaanxi Province of China [grant number 2015JQ6252]; the Ningbo Natural Science Foundation [grant numbers 2015A610109, 2015A610037 and 2016A610029]; and the Fundamental Research Funds for the Central Universities [grant number JB161405, JB161403].

References

[1] Jiaojiao Zhao, Yongping Pu, Yurong Wu, Panpan Zhang, J. Mater. Sci.: Mater. Electron. **26**(8), 6051 (2015).
[2] Hailong Li, Jianning Kang, Feng Guo, Yuanfang Qu, De'an Yang, Ceram. Int. **39**(7), 7589 (2013).
[3] Xingwen Zhu, Shengwei Wang, Shiwei Zhong, Yiyin Liu, Siyue Shen, Wenzhong Jiang, Xiao Zhou, Ceram. Int. **40**(8), 12383 (2014).
[4] V. Paunovic, V. V. Mitic, Lj. Kocic, Ceram. Int. **42**, 11692 (2016).
[5] M. M. Vijatović Petrović, J. D. Bobić, R. Grigalaitis, N. I. Ilic, A. S. Dzunuzovic, V. Jankauskaite, J. Banys, B. D. Stojanović, Ceram. Int. **41**, 11365 (2015).
[6] Gong Jian, Fu Xiaorong, Song Shigeng, Tan Hui, Tao Mingde, Chin. J. Semicon. **20**, 246 (1999).
[7] Shigeki Sato, Yukie Nakano, Akira Sato, Takeshi Nomura, J. Eur. Ceram. Soc. **19**(6-7), 1061 (1999).
[8] Masayoshi Yuasa, Takahito Nagano, Naoki Tachibana, Tetsuya Kida, Kengo Shimanoe, J. Am. Ceram. Soc. **96**, 1789 (2013).
[9] L. Affleck, J. Seaton, C. Leach, J. Eur. Ceram. Soc. **27**, 3439 (2007).
[10] Cao Minghe, Zhou Dongxiang, Gong Shuping, J. Funct. Mater. **3**, 341 (2001).
[11] W. Heywang, J. Am.Ceram. Soc. **47**, 484 (1964).
[12] J. Daniels, R. Wernicke, Philips Res. Rep. **31**, 544 (1976).
[13] G. H. Jonker, E. E. Havinga, Mater. Res. Bull. **17**, 345 (1982).
[14] S. B. Desu, D. A. Payne, J. Am. Ceram. Soc. **73**, 3407 (1990).
[15] Mingsheng Ma, Yilin Wang, Yiqing Lu, Wenjun Wu, Yongxiang Li, Ceram. Int. **41**, S804 (2015).
[16] Y. Pu, H. Wu, J. Wei, B. Wang, J. Mater. Sci: Mater. Electron. **22**, 1479 (2011).
[17] C. Leach, M. A. Zubair, Mat. Sci. Semicon. Proc. **15**, 47 (2012).
[18] M. A. Zubair, C. Leach, J. Eur. Ceram. Soc. **30**, 107 (2010).
[19] Huo Weirong, Liu Haohan, Liang Wei, Song Yuanqiang, Qu Yuanfang, Rare. Metal. Mat. Eng. **42**, 230 (2013).
[20] Qian Chen, Li Yong, Tang Xiaofeng, Tang Zilong, Qian Jin, Zhou Zhigang, J. Inorg. Mater. **16**, 734 (2001).
[21] Senlin Leng, Guorong Li, Liaoying Zheng, Tianbao Wang, Qingrui Yin, J. Am. Ceram. Soc. **92**, 2772 (2009).
[22] Ji Hun Jeong, Myung Gyu Park, Young Ho Han, J. Electroceram. **13**, 805 (2004).
[23] Zhang Daoli, Cao Minghe, Piezoelectric. Acoustic Opt. **22**, 40 (2000).
[24] Laxman Singh, III Won Kim, Byung Cheol Sin, Amir Ullah, Sang Kook Woo, Youngil Lee, Mat. Sci. Semicon. Proc. **31**, 386 (2015).
[25] J. R. Dygas, G. Fafilek, M. W. Breiter, Solid State Ionics **119**, 115 (1999).
[26] Pinghua Xiang, Hiroaki Takeda, Tadashi Shiosaki, J. Appl. Phys. **103**, 064102 (2008).

---

[*] Corresponding author: mlzhang@xidian.edu.cn